MERAL Publications and Solutions Pvt. Ltd.

Original Article

Doxycycline hyclate-loaded nanogels as a promising approach for dermal delivery

Layla Hammody Hashem[1], Ameerah A. Radhi[2]*

[1]Department of Pharmaceutics, College of Pharmacy, Al-Muthanna University, Al-Muthanna, Iraq. [2]Department of Pharmaceutics, College of Pharmacy, Al-Nahrain University, Baghdad, Iraq.

Correspondence: Ameerah A. Radhi, Department of Pharmaceutics, College of Pharmacy, Al-Nahrain University, Baghdad, Iraq. ameerah.abdulelah@nahrainuniv.edu.iq

Received: 03 June 2026; **Revised:** 29 August 2026; **Accepted:** 01 September 2026

ABSTRACT

Doxycycline hyclate is a broad-spectrum tetracycline- class antibacterial agent. It is available in 75 mg, 100 mg, and 150 mg delayed-release tablets for oral use, and widely prescribed in dermatology for treatment of acne vulgaris. Despite the favorable long-term track record of safety, the prolonged oral therapy usually applied in acne vulgaris is associated with side effects such as gastrointestinal side effects (i.e., esophagitis) and dose-related photosensitivity. To this end, it is essential to develop a topical formulation as an alternative to oral dosage forms. The purpose of this study is to formulate chitosan/hyaluronic acid nanogels for the topical delivery of doxycycline hyclate for the first time. The selected nanogel formula exhibited a hydrodynamic diameter and polydispersity index (PDI) of 196.25±1.65 nm and 0.168±0.016, respectively. In addition, it exhibited a positive surface charge (44±2.2 mV), which indicates adequate physical stability. With respect to *ex vivo* permeation, limited drug permeation was noticed within the first 12 hours of application onto mouse skin. Findings from antibacterial activity revealed an enhanced antibacterial effectiveness of doxycycline hyclate against *S. epidermidis* upon encapsulation of doxycycline hyclate into chitosan/hyaluronic acid nanogel. The selected formula exhibited excellent biocompatibility, maintaining cell viability above 90% across all tested concentrations, with no significant concentration-dependent cytotoxicity. Accordingly, doxycycline-loaded chitosan/hyaluronic acid nanogels appear to be promising for topical delivery and a potential alternative to the conventional tablet formulations.

Keywords: Doxycycline hyclate, Nanogels, Acne vulgaris, Antibacterial activity, Energy-dispersive X-ray

Introduction

Doxycycline hyclate is a broad-spectrum tetracycline- class antibacterial agent and is available in 75 mg, 100 mg, and 150 mg delayed-release tablets for oral use. Doxycycline hyclate is a water-soluble salt of the doxycycline base and has the molecular formula of $C_{22}H_{24}N_2O_8$, HCl, ½ C_2H_6O, ½ H_2O, and a molecular weight of 512.9 g/mole [1]. Doxycycline hyclate is indicated for urinary, intestinal, respiratory, ocular, dental, dermatological, and sexually transmitted infections. Additionally, it is indicated as adjunctive therapy in acute intestinal amebiasis and severe acne [2].

Acne vulgaris is a common cutaneous disorder that is inflammatory in nature and caused by complex pathologic events, involving increased sebum production, follicular hyperkeratinization, proliferation of bacteria, most frequently *Cutibacterium acnes* (*C. acnes*) and *Staphylococcus epidermidis* (*S. epidermidis*) in pilosebaceous units, and local inflammatory cascades. The management of moderate to severe acne vulgaris usually involves prolonged oral doxycycline therapy over several weeks to months. Although doxycycline has a favorable long-term track record of safety, it is associated with effects that might negatively impact patient compliance and clinical outcomes. Among the reported side effects are gastrointestinal side effects (i.e., esophagitis) and dose-related photosensitivity [3]. These

Access this article online	
Website: www.japer.in	**E-ISSN:** 2249-3379

How to cite this article: Hashem LH, Radhi AA. Doxycycline hyclate-loaded nanogels as a promising approach for dermal delivery. J Adv Pharm Educ Res. 2026;16(3):151-60. https://doi.org/10.51847/ktZvvR9ySs

This is an open access journal, and articles are distributed under the terms of the Creative Commons Attribution-Non Commercial-ShareAlike 4.0 License, which allows others to remix, tweak, and build upon the work non-commercially, as long as appropriate credit is given and the new creations are licensed under the identical terms.

limitations can be overcome by nano-based platforms for dermal delivery, as they offer enhanced permeation and targeting of the skin pilosebaceous units where bacterial colonies reside. Additionally, nanocarriers protect their loaded drug molecules and minimize environmental stability issues [4].

A nanogel (nanohydrogel) is a nano-sized hydrogel, defined as a three-dimensional network of crosslinked hydrophilic polymers with an ability to swell by holding a large amount of water while maintaining the structure [5, 6]. Nanogels possess desirable attributes to be promising delivery systems for dermal and transdermal delivery. Nanogels are hydrophilic in nature, boost the hydration of the stratum corneum, and cause formation of channels for enhanced skin penetration. In addition, the release of the encapsulated medicinal agents can be tailored to be responsive to stimuli such as temperature, light, pH, or enzymes [7].

Chitosan (CS) is a linear polysaccharide produced by deacetylation of chitin and is composed of D-glucosamine and N-acetyl-D-glucosamine units. By harnessing its cationic nature due to the presence of amino groups, chitosan is employed to formulate nanogel via electrostatic attraction with negatively charged polymers. Besides, chitosan boosts skin permeability through its interaction with the negatively charged membranes of the epithelial cells [7, 8]. Hyaluronic acid (HA), on the other hand, is a linear polysaccharide, an anionic glycosaminoglycan, consisting of disaccharide units of D-glucuronic acid and N-acetyl-D-glucosamine. HA is a natural component of the extracellular matrix in the skin, resembling a sponge to retain water and provide elasticity. Thus, it is widely employed in dermatology as a major component in nanoplatforms and as a permeation enhancer owing to its hydration property. Additionally, carboxylic acid groups in HA facilitate nanogel formulation via electrostatic interactions with cationic polymers [9].

Both chitosan and hyaluronic acid are biocompatible, non-toxic, and biodegradable. Given that, we hypothesize that encapsulation of doxycycline hyclate into chitosan/hyaluronic acid nanogel offers an alternative to the conventional oral therapy. The present study aims to design chitosan/hyaluronic acid nanogels for topical delivery of doxycycline hyclate and evaluate their physico-chemical characteristics, antibacterial activity, cytotoxicity, and *ex vivo* skin permeation and disposition.

Materials and Methods

Materials

Doxycycline hyclate was purchased from Meyer, China; chitosan (low molecular weight was purchased from Central Drug House (P) Ltd., India; hyaluronic acid (250 kDa) was purchased from Tunchem Pharm (Shanghai) Tech Co., China. Sodium tripolyphosphate (TPP) was purchased from Himedia Laboratories Pvt. Ltd., India; 3-(4,5-Dimethyl-2-thiazolyl)-2,5diphenyl-2H-tetrazolium bromide (MTT) was purchased from Ambeed, USA.

Methods

Formulation of blank and doxycycline hyclate-loaded nanogels

Blank nanogel formulations were prepared using the ionic gelation technique. Briefly, chitosan was dissolved in 0.1N acetic acid solution at a concentration of 5 mg/mL. Hyaluronic acid (250 kDa) was dissolved in distilled water (D.W) at a concentration of 1 mg/mL. The cross-linking agent, sodium tripolyphosphate (TPP), was also dissolved separately in D.W. at a concentration of 20 mg/mL. Thereafter, the polyanion phase, comprised of HA and TPP solutions, was added dropwise into chitosan solution under magnetic stirring at 200 rpm for about 60 minutes. At this stage, the solution turned turbid (characteristic Tyndall effect), implying nanogel formation. Then, the nanogel formulations were probe sonicated for 20 seconds. Different formulations were prepared by altering the mass ratio of chitosan and TPP while HA concentration was kept constant **(Table 1)**. Loaded nanogel formulations were prepared using the same method, but including doxycycline hyclate in the chitosan solution [10].

Table 1. Composition of blank and doxycycline hyclate-loaded nanogels

Formula code	Chitosan (mg/mL)	TPP (mg/mL)	Hyaluronic acid (HA) (mg/mL)	Chitosan: TPP: HA mass ratio	Drug: carrier ratio
F1	2.5	2.5	0.125	1:1:0.05	----
F2	2.5	5	0.125	1:2:0.05	----
F3	2.5	1.25	0.125	1:0.5:0.05	-----
F4	2.5	5	0.125	1:2:0.05	1:2
F5	2.5	5	0.125	1:2:0.05	1:4

Characterization of blank and doxycycline hyclate-loaded nanogels

Dynamic light scattering (DLS)

Determination of the hydrodynamic diameters and size distribution (polydispersity index) of nanogels was performed by a dynamic light scattering system (DLS) using a 90Plus Particle Size Analyzer (Brookhaven Instruments Corporation, USA). Each sample was diluted with an equal volume of distilled water (DW) and analyzed at a temperature of 25^{0}C [11].

Determination of zeta potential (ζ)

Zeta potential (ζ) is a measure of the surface charge of the prepared nanogels. It was determined by the laser Doppler microelectrophoresis technique using a Zeta Plus zeta potential analyzer (Brookhaven Instruments Corporation, USA). Each

sample was diluted properly with distilled water (DW) and analyzed at a temperature of 25ºC [12].

Field emission scanning electron microscopy (FESEM)

The morphology of doxycycline hyclate-loaded nanogel (selected formula) was examined by means of Field Emission Scanning Electron Microscopy (FESEM) (Inspect TM F50, FEI company, USA). Samples were allowed to dry at room temperature on a glass slide, then coated with gold under vacuum to make them electrically conductive. Thereafter, samples were examined by FESEM, with an accelerating voltage from 200 V to 30 kV [13].

Ex-vivo studies

Ex vivo studies were undertaken with approval of the ethical committee in the College of pharmacy/Al-Nahrain University (nah.c.pha.41). The skin was obtained from healthy male Swiss albino BALB/c mice (n = 3) with an average weight of 25 g, kept under 12 hours light/dark cycle at 25±2°C with free access to water and food. The hair was shaved, mice were sacrificed, and then dorsal skin was harvested.

Permeation and skin disposition assessments

Ex vivo permeation was performed for doxycycline hyclate-loaded nanogel (selected formula) using a vertical Franz cell with an effective permeation area of 4.91cm2. In brief, skin was hydrated with D.W. for about one-hour prior use, and mounted between the donor and receptor compartments, where the stratum corneum faced the donor compartment. Then, a quantity of formulation equivalent to 1 mg of doxycycline hyclate was placed in the donor compartment. The receptor compartment comprised 35 mL of phosphate-buffered saline PBS (pH 7.4), and the entire device was maintained at a constant temperature of 37°C ±0.5 °C and a constant stirring speed of 100 rpm. Then, at specified time intervals (1,2,4,8,12 and 24 hours), 1-mL samples were collected from the receptor and replaced immediately with an equal volume of pre-heated PBS. Sample solutions were protected from light and stored at 4°C until analysis by High-Performance Liquid Chromatography (HPLC). After a 24-hour duration, whole skin was removed from franz cell, and the surface was cleaned with filter paper soaked with DW and dried thoroughly. In order to remove the stratum corneum, nine strips of adhesive Scotch tape were used, which were then soaked in methanol to obtain the amount of drug deposited in this layer. The remaining skin, which comprised viable epidermis and dermis, was cut into small pieces, soaked in methanol overnight, ultrasonicated, and centrifuged for complete extraction of the drug, followed by filtration. The filtrates were then assayed by HPLC. All measurements in this study were conducted in triplicate [14].

HPLC assay

The method employed for the quantification of doxycycline hyclate was adapted from previous study by Elshater *NS et al.* using mobile phase composition: acetic acid 5%: acetonitrile: methanol 55:25:20. The method was conducted using (Azura ASM 2.1L, KNAUER, Germany) HPLC instrument and reversed-phase column C18 (4.6IDx250 mm) in isocratic elution at 1 mL/ minute flow rate, injection volume of 25 µL, temperature of 25°C and total duration for each run of 10 minutes. A calibration curve for doxycycline hyclate was constructed by dissolving the drug in methanol and preparing serial dilutions detected at a UV wavelength of 347 nm [15].

Antibacterial activity

Evaluation of antimicrobial activity using the alamar blue assay

The antibacterial activity of doxycycline hyclate-loaded nanogel (selected formula) or aqueous doxycycline hyclate solution was evaluated against *S. epidermidis* using the alamar blue assay. Alamar blue is a redox indicator that exhibits a color change with the proliferation state of bacterial cells. It is blue-colored in its oxidized state and changes color in response to cellular metabolic reduction to the red (reduced state) [16].

In order to determine the values of minimum inhibitory concentration (MIC), serial dilutions of nanogel and doxycycline hyclate solution were prepared in sterile Mueller-Hinton Broth (MHB). Then, 150 µL of each concentration was added into a sterile 96-well plate, followed by 50 µL of bacterial suspension, in triplicate. The plates were incubated at 37 °C for 24 hours under aerobic conditions. Subsequently, alamar blue reagent was added to the wells, and the plates were further incubated in the dark at 37 °C for 2 hours. The MIC was then determined visually as the lowest concentration at which the well displayed a completely blue color, indicating total inhibition of bacterial growth [17].

The half-maximal inhibitory concentration (IC_{50}) was determined by exposing a standardized bacterial suspension (10^5 CFU/mL) to serial dilutions of nanogel and doxycycline hyclate, followed by incubation at 37°C for 24 hours. Bacterial growth was measured spectroscopically at 600 nm, and the IC_{50} value was calculated as the concentration that inhibited 50% of bacterial growth compared to the untreated control. The dose-response curve and IC_{50} were obtained using GraphPad Prism software, version 9.0 [18].

Evaluation of antimicrobial activity using the well-diffusion method

Bacterial suspensions were adjusted to the 0.5 McFarland standard and spread evenly on Mueller-Hinton agar (MHA) plates. Wells of 6 mm diameter were aseptically punched into the agar. Then, 100 µL of doxycycline hyclate-loaded nanogel (selected formula) or aqueous doxycycline hyclate solution at different concentrations (5 mcg/mL and 20 mcg/mL) were

added into each well and incubated at 37°C for 24 hours. Thereafter, zones of inhibition were measured in millimeters. All experiments were carried out in triplicate [19].

In vitro cytotoxicity using the MTT assay

The safety and biocompatibility of doxycycline hyclate-loaded nanogel (selected formula) was assessed in mouse L929 fibroblast cells. Cells were exposed to different concentrations (0.62– 20 µg/mL) of doxycycline hyclate-loaded nanogel or aqueous doxycycline hyclate solution for 48 hours duration.at 37°C. MTT solution was then added into wells and further incubated for 4 hours. Thereafter, supernatants were removed, and the resulting formazan crystals were dissolved with DMSO, and the optical density of the wells was examined using a microplate reader at 570 nm [20].

Fourier transform infrared spectroscopy (FTIR)

Samples of pure doxycycline hyclate, chitosan, hyaluronic acid, TPP, and doxycycline hyclate-loaded nanogel (selected formula) were ground into fine powders, mixed with potassium bromide, and pressed into discs. FT-IR spectra were recorded in the range of 4000–400 cm^{-1} using an FT-IR spectrometer (Shimadzu, Japan) [21].

Analysis by SEM and energy-dispersive X-ray (EDS)

A sample of doxycycline hyclate-loaded nanogel (selected formula) was examined using (Axia™ ChemiSEM, Thermo Scientific™) to obtain information on the elemental makeup of the sample at an acceleration voltage of 30 kV.

Statistical analysis

Data are expressed as the mean ± SD. One-way analysis of variance (ANOVA) with Tukey's post-test was carried out to evaluate significance ($p < 0.05$) using GraphPad Prism version 9 (GraphPad Software LLC, San Diego, CA, USA).

Results and Discussion

Chitosan/hyaluronic acid nanogel formulas were prepared by the ionic gelation technique. This technique is based on the electrostatic interaction that occurs spontaneously between the protonated amine groups of chitosan solution and the anionic carboxylate and phosphate groups of hyaluronic acid /TPP solution [22, 23].

Firstly, three blank nanogel formulas (F1-F3) were prepared at different (chitosan: TPP: HA) mass ratios to study the effect of crosslinker concentration on the physicochemical properties of the prepared nanogels, while keeping chitosan and hyaluronic acid concentrations constant. The hydrodynamic diameters of the prepared nanoparticles were monitored using the DLS technique.

It was observed that the formula F2 containing the highest concentration of TPP among the three formulas had a significantly ($p < 0.05$) smaller diameter (202.45 ±25.8 nm), as presented in **Table 2**. The polyanion, sodium tripolyphosphate (TPP, is a negatively charged crosslinker that can interact with chitosan chains through non-covalent crosslinking. Therefore, a high concentration of TPP anion can generate a more condensed polymeric network and smaller particle-size nanogels [24].

Zeta potential (ζ) values represent the surface charge of the nano-formulation and indicate the stability of the formulation. As shown in **Table 2**, the values were positive, except in F1, suggesting the predominance of protonated amine groups of chitosan on the surface of the nanogel formulation [11]**.** The negative charge for formula F1 might be due to the adsorption of negatively charged HA or TPP to the surface. Based on the above observations, formula F2 was selected for drug loading.

Next, nanogel formulas F4 and F5 were prepared to study the influence of drug loading at drug-to-carrier ratios (1:2) and (1:4), respectively, on the particle size of the prepared nanogels. Compared to the blank formula (F2), a non-significant decrease ($p>0.05$) in mean particle diameter was observed in F4 and F5. It was also found that changing the drug: carrier ratio from (1:2) in F4 to (1:4) in F5 caused a non-significant ($p> 0.05$) increase in mean particle diameter.

Size reduction upon doxycycline hyclate loading can be interpreted by different mechanisms. Firstly, drug molecules can intercalate between polymer chains, acting as crosslinkers, preventing polymer chains from swelling. Secondly, the hydrophobic portion of the drug might decrease water entry into the polymer chains and inhibit further polymer swelling, resulting in more compact structures [25].

Comparing zeta potential (ζ) in F4 to the blank nanogel formula F2, the significant ($p<0.05$) reduction in the magnitude of zeta potential (ζ) upon drug loading can be explained by the negative charge of hyclate anions neutralizing the positive charge of amino groups of chitosan. Formula F5, on the other hand, prepared at a drug: carrier ratio (1:4), exhibited a zeta potential (ζ) of 44±2.2 mV, which provides a strong electrostatic repulsion barrier and adequate physical stability [26]. Besides, F5 exhibits a particle diameter of 196.25±1.65 nm and a polydispersity index (PDI) of 0.168±0.016, suggesting a monodisperse system. Therefore, based on the above data, formula F5 was chosen to perform further analyses.

Table 2. The Physicochemical Properties of Blank and Doxycycline Hyclate - Loaded Nanogels

Formula code	Particle diameter (nm)	Polydispersity (PDI)	Zeta potential (mV)
F1	408.3±8.48	0.369± 0.077	-68.17±3.408
F2	202.45±25.8	0.551±0.129	38.04±1.902
F3	299.7±23.6	0.504±0.033	15.67±0.123
F4	154.2±32.2	0.125±0.115	2.335±0.705
F5	196.25±1.65	0.168±0.016	44±2.2

Field emission scanning electron microscopy (FESEM)

FESEM micrographs of doxycycline hyclate-loaded nanogel (F5) **(Figures 1a and1b)** show high agglomeration of nanoparticles in the dry state. However, nanogels show an almost spherical shape in the nanosized range [27]. Additionally, they exhibit rough or porous surfaces, typical for hydrogels, usually resulting from the crosslinking process [28]. When observed under AFM **(Figure 1c)**, the resulting images were consistent with FESEM micrographs.

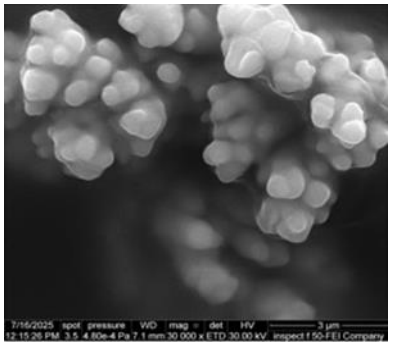

a)

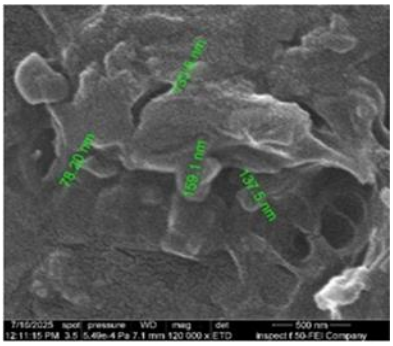

b)

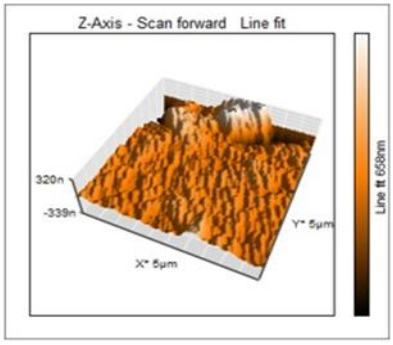

c)

Figure 1. (a and b): FESEM images of F5. (c): AFM image of F5

Ex vivo studies

Permeation and skin disposition assessments

Ex vivo permeation and skin disposition analyses were examined for doxycycline hyclate-loaded nanogel (F5). Following a 24-hour duration of the experiment, the amount of doxycycline hyclate retained in the mouse skin (viable epidermis and dermis) was found 11.789± 2.4 percent **(Table 3)**, while no detectable amount of drug was found in the stratum corneum.

With respect to drug permeation, it was observed that during the first 12 hours of the experiment, no amount of drug was detected in the receptor compartment, suggesting limited permeation through the skin. Interestingly, after 24 hours, 21.74±5.2 percent of doxycycline was detected [29-35]. The molecules of doxycycline hyclate are water-soluble; thus, their penetration across the stratum corneum represents a significant obstacle. Upon encapsulation into chitosan/hyaluronic acid nanogel, skin permeation can be enhanced due to electrostatic interactions between positively charged chitosan and the negatively charged skin, promoting both transcellular and paracellular transport of drug across the skin [36].

Table 3. Results of *Ex-Vivo* Permeation and Skin Disposition Assessments

Formula Code	Percent drug permeated after 24 hours	Percent drug deposited in skin (viable epidermis and dermis) after 24 hours
F5	21.74±5.2	11.789± 2.4

Antibacterial activity

Doxycycline hyclate is a tetracycline-class antimicrobial agent, primarily bacteriostatic. The antibacterial effect is attributed to the inhibition of bacterial protein synthesis by binding to the 30S ribosomal subunit and blocking the association of the charged aminoacyl-tRNA (aa-tRNA) with the ribosomal A site. The antibacterial test findings imply enhanced antibacterial effectiveness of doxycycline hyclate against *S. epidermidis* upon encapsulation of doxycycline hyclate in chitosan/hyaluronic acid nanogel [37-45]. Formulation F5 exhibited a significantly ($p<0.05$) lower MIC and IC_{50} (5.2±0.26 and 10±0.6 mcg/mL) than those of doxycycline hyclate solution (6.5±0.325 and 12±0.72), respectively. Furthermore, doxycycline hyclate-loaded nanogel (F5) exhibited a higher zone of inhibition than that of doxycycline hyclate solution, as demonstrated in **Figure 2.** Similar findings have been reported for doxycycline-loaded niosomal gels, thymol-loaded chitosan nanogels, and carboxymethyl chitosan lysozyme nanogels loaded with tea polyphenols, silver nitrate ($AgNO_3$), and chlorhexidine [3, 46, 47].

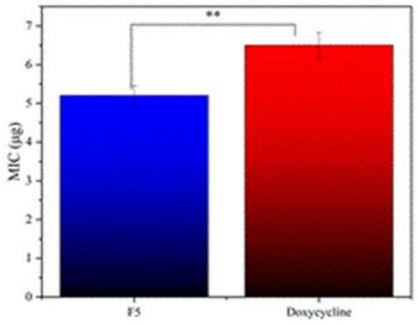

a)

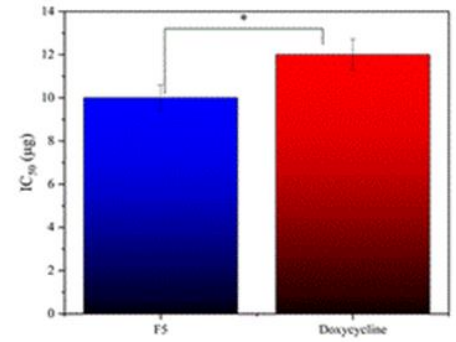

b)

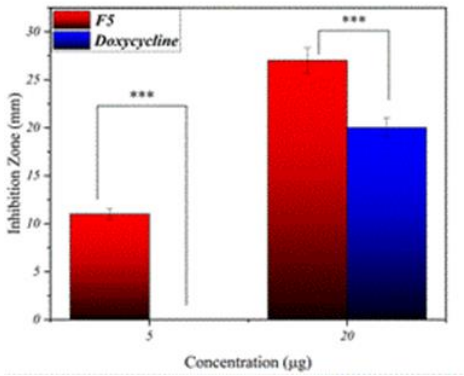

c)

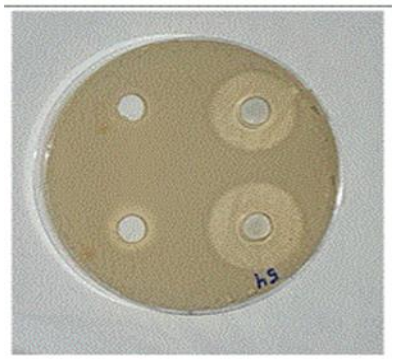

d)

Figure 2. a) Minimum inhibitory concentration (MIC) of nanogel (F5) and doxycycline hyclate solution, b) Half maximal inhibitory concentration (IC50) of nanogel (F5) and doxycycline hyclate solution, c&d) Zones of inhibition of nanogel (F5) and doxycycline hyclate solution against *S. epidermidis*

In vitro cytotoxicity using the MTT assay

Figure 3a shows the cell survival percentage of L929 fibroblast cells after 48 hours of treatment with doxycycline hyclate-loaded nanogel (F5) relative to the DMSO-treated control. Based on the data obtained, it can be concluded that F5 exhibited excellent biocompatibility, maintaining cell viability above 90% across all tested concentrations (0.62–20 µg/mL), with no significant concentration-dependent cytotoxicity. In contrast, doxycycline hyclate solution exhibited a concentration-dependent decrease in cell viability, with minimal cytotoxicity at low concentrations (0.62–5 µg/mL) and a marked reduction in cell survival at higher concentrations (10–20 µg/mL) and a half-maximal inhibitory concentration (IC_{50} = 9.36 µg/mL) **(Figures 3b and 3c).** Drug encapsulation in chitosan/hyaluronic acid nanogel formulation minimized the direct contact of doxycycline with the cells, rendering the formulation safe for topical application. Similar observations have been reported by Della Sala *et al.* and Simpson *et al.* [22, 48].

Reasons for biocompatibility arise from the biocompatible ingredients in the formulation, where hyaluronic acid is a natural constituent in the connective tissue of skin [49-55]. Chitosan, on the other hand, is a natural biopolymer with a positive impact on the growth of normal skin fibroblasts, as reported by Gao *et al.* [56]. Additionally, the safety and biocompatibility of TPP are proven and documented in the literature [57].

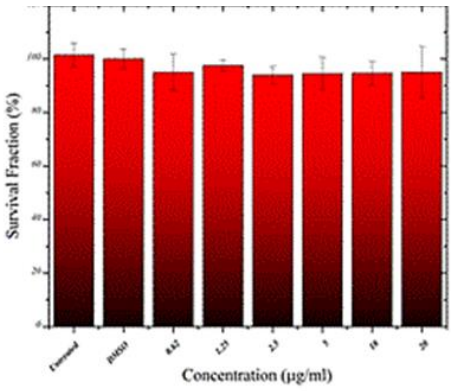

a)

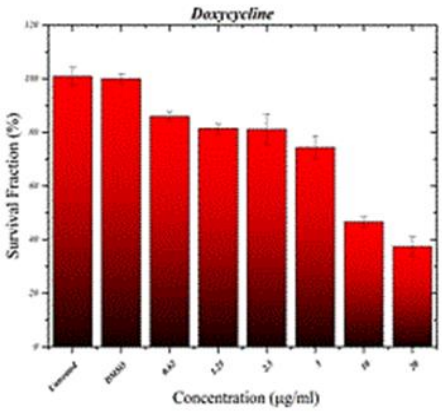

b)

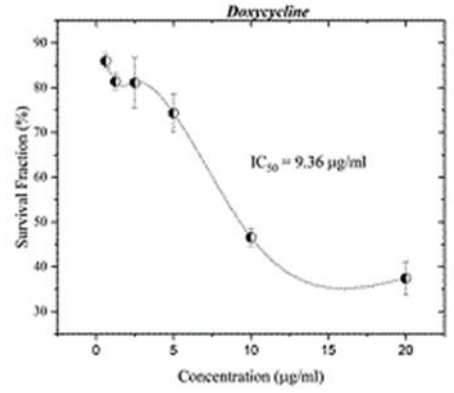

c)

Figure 3. a) Effect of F5 on the viability of L929 fibroblast cells after 48 h of treatment, as determined by the MTT assay. Cell survival fraction (%) is expressed relative to the DMSO-treated control (100%). Data are presented as mean ± SD from independent experiments. b) Effect of doxycycline on the

viability of L929 fibroblast cells after 48 h of treatment, as determined by the MTT assay. c) Dose–response curve showing the effect of doxycycline on L929 fibroblast cell viability after 48 h of treatment, as determined by the MTT assay. Cell survival fraction (%) was plotted against doxycycline concentration (0.62–20 µg/mL), and the data were fitted using nonlinear regression to estimate the half-maximal inhibitory concentration (IC_{50} = 9.36 µg/mL). Data are presented as mean ± SD from independent experiments.

Fourier transform infrared spectroscopy (FTIR)

FT-IR spectra of doxycycline hyclate, chitosan, HA, TPP, and doxycycline hyclate-loaded nanogel (F5) are shown in **Figure 4a.** FT-IR spectrum of doxycycline hyclate shows N-H stretching vibrations of primary amides: asymmetrical stretching at 3452.58 cm^{-1} and symmetrical stretching at 3332.99 cm^{-1}, overlapped with O-H stretching vibrations in the same range; an absorption band at 1678.07 cm^{-1} due to C=O stretching (amide I band), absorption band at 1614.42 cm^{-1} corresponding to N-H bending vibrations (amide II) [58].

FT-IR spectrum of chitosan showed multiple bands in the range 3200-3500 cm^{-1} attributed to overlapped stretching vibrations of N-H and O-H; a band at 2872.01 cm^{-1} reflecting symmetric C-H stretching vibrations of the methylene group commonly observed in the spectra of polysaccharides. Additionally, an absorption band was detected at 1654.92 cm^{-1} mainly attributed to C=O stretching (amide I band) due to the residual N-acetyl groups present in chitosan, and a band at 1560.41 cm^{-1} attributed to N-H bending (amide II) [59].

In the spectrum of sodium tripolyphosphate, a broad band was observed in the range of 3000-3200 cm^{-1} corresponding to OH stretching because the sample was provided in hydrated form. In addition, distinct bands corresponding to the stretching vibration of P=O, PO_2, and PO_3 groups in TPP appeared at 1041.56, 1010.70, and 972.12 cm^{-1} (26). The spectrum of hyaluronic acid shows peaks at 3460.30 cm^{-1} corresponding to O-H stretching vibration; 2891.30 cm^{-1} due to C-H stretching; and 1647.21 cm^{-1} due to C=O stretching vibration. In addition, both amide I (C=O stretching) and amide II (N-H bending) bands appear at 1622.13 and 1556.55 cm^{-1}, respectively [60].

In the spectrum of doxycycline hyclate-loaded nanogel (F5), it can be observed that C=O stretching (amide I band) and N-H bending vibrations (amide II) of doxycycline hyclate have shifted to lower frequencies to 1645.28 and 1587.42 cm^{-1}, suggesting the involvement of doxycycline in hydrogen bonding or electrostatic attraction with polymer chains or the crosslinking agent [61-66]. On the other hand, bands corresponding to the phosphate group in TPP have disappeared, while the characteristic bands of chitosan related to amide I (C=O stretching) and amide II (N-H bending) have shifted to lower frequency, with similar observations for hyaluronic acid. These observations confirm the bonding undertaken between phosphate groups in TPP and amino groups in chitosan and/or hyaluronic acid chains [22, 60].

Analysis by SEM and energy-dispersive X-ray (EDS)

The results of EDS provide elemental mapping of the sample. It can be observed **(Figure 4b)** that the sample consists of C, N, O, Na, P, and CL. The presence of Na and P implies the presence of sodium tripolyphosphate in the structure of the nanogel formula, while C, N, and O are constituents of chitosan, hyaluronic acid, and doxycycline hyclate. On the other hand, CL implies the presence of drug molecules since it is only present in the structure of doxycycline hyclate. This study confirms the formation of nanogel and incorporation of drug molecules within its structure [67].

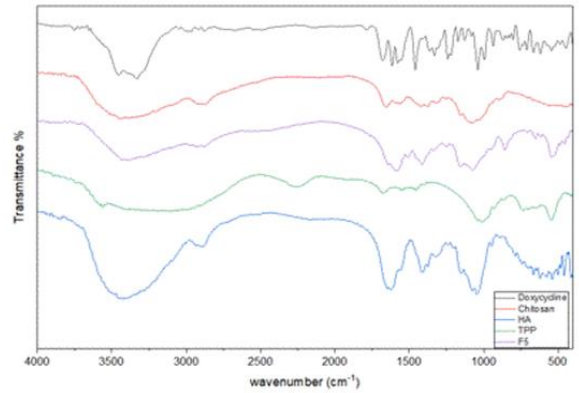

a)

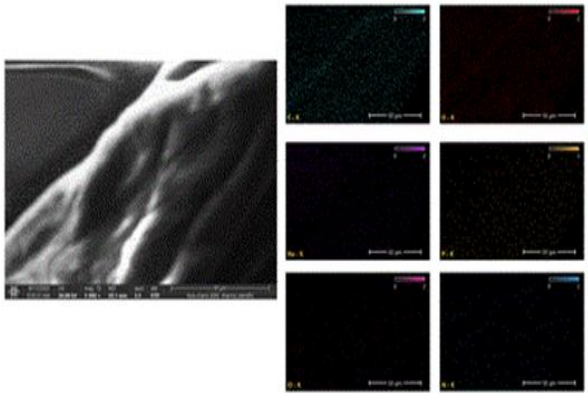

b)

Figure 4. a) FTIR spectra of doxycycline hyclate, chitosan, hyaluronic acid, sodium tripolyphosphate (TPP), doxycycline hyclate-loaded nanogel (F5), b) EDS mapping of doxycycline hyclate loaded nanogel (F5)

Conclusion

Based on the results obtained, chitosan/hyaluronic acid nanogels were successfully prepared by the ionic gelation technique. The prepared nanogels were in the nanosized range suitable for topical delivery, with enhanced antibacterial activity and biocompatibility. Chitosan/hyaluronic acid nanogels might represent a promising approach for dermal delivery, though further investigations are required. These investigations include

evaluating the antimicrobial activity against other bacterial strains; incorporating the nanogel formulation into semisolid vehicles and studying their rheological properties, spread ability, and *ex vivo* permeation; stability studies; and *in vivo* studies.

Acknowledgments: The authors acknowledge the College of pharmacy/Al-Nahrain University, Baghdad College of Medical Sciences, Center of Nanotechnology and Advanced Research/University of Technology, and Al-Razi Center for Research and Diagnostic Kit Production for their assistance in accomplishing this research.

Conflict of interest: None

Financial support: None

Ethics statement: *Ex vivo* studies were undertaken under the approval of the ethical committee in the College of pharmacy/Al-Nahrain University (nah.c.pha.41).

References

1. The Japanese Pharmacopoeia. 15th ed. Tokyo: Society of Japanese Pharmacopoeia; distributed by Yakuji Nippo; 2006. p. 606-8.
2. Del Rosso JQ. Oral doxycycline in the management of acne vulgaris: current perspectives on clinical use and recent findings with a new double-scored small tablet formulation. J Clin Aesthet Dermatol. 2015;8(5):19-26.
3. Alkilani AZ, Sharaire Z, Hamed R, Basheer HA. Transdermal delivery system of doxycycline-loaded niosomal gels: toward enhancing doxycycline stability. ACS Omega. 2024;9:33542-56. doi:10.1021/acsomega.4c01224
4. Feitosa RC, Ishikawa ESA, da Silva MFA, da Silva-Junior AA, Oliveira-Nascimento L. Five decades of doxycycline: does nanotechnology improve its properties? Int J Pharm. 2022;618:121655.
5. Siafaka PI, Ozcan Bulbul E, Okur ME, Karantas ID, Ustundag Okur N. The application of nanogels as efficient drug delivery platforms for dermal/transdermal delivery. Gels. 2023;9:753. doi:10.3390/gels9090753
6. Liu Y, Al-Hakeem M, Abdulrazzaq, Almajidi YQ, Yaseen A. Engineering of glycyrrhizin-loaded chitosan nanogel for pulmonary immunomodulation via regulation of NF-kB signaling and macrophage polarization in lung inflammation. Int J Biol Macromol. 2026;362:152117.
7. Radeva L, Yoncheva K. Nanogels—innovative drug carriers for overcoming biological membranes. Gels. 2025;11:124. doi:10.3390/gels11020124
8. Mohite P, Rahayu P, Munde S, Ade N, Chidrawar VR, Singh S, et al. Chitosan-based hydrogel in the management of dermal infections: a review. Gels. 2023;9:594. doi:10.3390/gels9070594
9. Matalqah S, Lafi Z, Asha SY. Hyaluronic acid in nanopharmaceuticals: an overview. Curr Issues Mol Biol. 2024;46:10444-61. doi:10.3390/cimb46090621
10. Manivong S, Garcia AC, Patten SA, Fernandes JC, Benderdour M, Banquy X, et al. Chitosan-based nanogels: synthesis and toxicity profile for drug delivery to articular joints. Nanomaterials. 2022;12:1337. doi:10.3390/nano12081337
11. Saleem K, Siddiqui B, ur-Rehman A, Shah KU, Ahmed N. Minoxidil nano-hydrogel based on chitosan and hyaluronic acid for potential treatment of androgenic alopecia. Bionanoscience. 2025;15(2):258. doi:10.1007/s12668-025-01870-1
12. Sidhavatam H, Reddy MV. Formulation and development of doxycycline hyclate loaded chitosan nanoparticles crosslinked topical hydrogel patches for healing diabetic foot ulcer. J Med Chem Sci. 2024;7:753-76. doi:10.26655/JMCHEMSCI.2024.6.1
13. Radhi AA, Ali WK, Al-Saedi F. Preparation and in vitro evaluation of synthetic high-density lipoproteins as a parenteral drug delivery system for tamoxifen citrate. Iraqi J Pharm Sci. 2023;32(3):105-17. doi:10.31351/vol32iss3pp105-117
14. Kashani-Asadi-Jafari F, Hadjizadeh A. Niosome encapsulated doxycycline-hyclate for potentiation of acne therapy: formulation and characterization. Pharm Nanotechnol. 2022;10(1):56-68.
15. Elshater NS, Hussein F, Fadel MA, Ragab M, Hassan H, Sabry M. Validation of HPLC method for determination of doxycycline hyclate in turkey serum. Egypt J Chem Environ Health. 2016;2(2):282-91.
16. Calvo LG, Castillo A, Villarino RA, Rama JLR, Abril AG, de Miguel T. Study of the antibacterial activity of rich polyphenolic extracts obtained from *Cytisus scoparius* against foodborne pathogens. Antibiotics (Basel). 2023;12(11):1645. doi:10.3390/antibiotics12111645
17. Ojha DK, Mehra A, Rout SS, Giri S, Nayak S. Bactericidal activity of ZnO nanoparticles-anti-TB drug combination towards the H37Rv strain and multidrug-resistant isolates of Mycobacterium tuberculosis via SufB splicing inhibition. Mater Adv. 2025;6:5242-59. doi:10.1039/d4ma01224k
18. Achieng AO, Ingasia LA, Juma DW, Cheruiyot AC, Okudo CA, Yeda RA, et al. Reduced in vitro doxycycline susceptibility in Plasmodium falciparum field isolates from Kenya is associated with PfTetQ KYNNNN sequence polymorphism. Antimicrob Agents Chemother. 2014;58(10):5894-9. doi:10.1128/aac.02788-13
19. Mostafa EM, Badr Y, Hashem MM, Abo-EL-Sooud K, Faid AH. Reducing the effective dose of doxycycline using chitosan silver nanocomposite as a carrier on Gram-positive and Gram-negative bacteria. Sci Rep. 2024;14(1):27819. doi:10.1038/s41598-024-78326-1
20. Dubey P, Kumar A, Vaiphei KK, Basrani S, Jadhav A, Wilen CE, et al. A poly-δ-decalactone (PDL) based nanoemulgel for topical delivery of ketoconazole and eugenol against Candida albicans. Nanoscale Adv. 2024;6(21):5322-36.

21. Almajidi Y, Abdullaev S, Alani B, Saleh E, Ahmad I, Ramadan M, et al. Chitosan-gelatin hydrogel incorporating polyvinyl alcohol and MnFe double-layered hydroxide nanocomposites with biological activity. Int J Biol Macromol. 2023;246:125566.
22. Della Sala F, Barretta M, Di Gennaro M, Paradiso R, Borriello G, Borzacchiello A. Bio-composite nanogels based on chitosan and hyaluronic acid for the treatment of lung infections. Gels. 2024;10(11):709. doi:10.3390/gels10110709
23. Ali Mujtaba M, Alotaibi NM. Formulation and evaluation of chitosan-based nanogel for oral delivery of diosmin. Pak J Pharm Sci. 2023;36(2):535-540.
24. Hassan UA, Hussein Z, Masarudin MJ. Synthesis of a nanoparticle system for the enhanced accumulation of fluorescently-labelled amino acids encapsulated in monodispersed chitosan nanoparticle system. Malays Appl Biol. 2017;46(1):171-5.
25. Sadoun-Daikha O, González Rodríguez ML, Azouz LH, Rabasco AM, Rezgui F. Central composite design optimization for a controlled valsartan release from polycaprolactone microspheres. J Appl Polym Sci. 2022;139(5):e51584. doi:10.1002/app.51584
26. Darwish AB, Mohsen AM, Elshebiney S, Elgohary R, Younis MM. Development of chitosan lipid nanoparticles to alleviate the pharmacological activity of piperine in the management of cognitive deficit in diabetic rats. Sci Rep. 2024;14:8247.
27. Bozorgi A, Haghighi Z, Khazaei MR, Bozorgi M, Khazaei M. The anti-cancer effect of chitosan/resveratrol polymeric nanocomplex against triple-negative breast cancer: an in vitro assessment. IET Nanobiotechnol. 2023;17(2):91-102. doi:10.1049/nbt2.12108
28. Hakkoymaz O, Mazi H. Both pH and temperature-sensitive copolymer nanogels for controlled release of doxorubicin. Polym Bull. 2025. doi:10.1007/s00289-025-05880-7
29. Thuy NV. Developing management information systems creates competitive advantages for businesses. J Organ Behav Res. 2025;10(1):15-9. doi:10.51847/YMdKnN15u3
30. Asif S, Shahbaz MS. Project success through organizational climate and work behavior: systematic literature review. J Organ Behav Res. 2025;10(1):1-14. doi:10.51847/cUhkprt6DJ
31. Maleckaite G, Mockeviciute D, Jonusas R. Modern radiological diagnostic methods for oral mucosal melanoma: recent advances and future perspectives. Ann Dent Spec. 2025;13(1):7-12. doi:10.51847/orYhE8CnY5
32. Al-Sunbul AA, Aldhalaan R, AlHaddab M, AlRushoud SS, Alharbi M. Multidisciplinary course of action in treating an intricate dental condition: a case report. Ann Dent Spec. 2025;13(1):1-6. doi:10.51847/tMCyhI2l0C
33. Narayana AV, Kumar P, Sumalatha B, Chandrasekhar K, Rao AR, Rashmika I. Biosurfactants as key agents in microbial remediation of polycyclic aromatic hydrocarbons: a review. J Biochem Technol. 2025;16(1):9-14. doi:10.51847/TImJVEmxU3
34. Ati UB, Atangwho IJ, Itam EH. Effect of monosodium glutamate on selected tissue lipids and haematology of neonatal and adult Wistar rats. J Biochem Technol. 2025;16(1):1-8. doi:10.51847/88vnUSGDHJ
35. Fritea L, Fodor R, Bei MF, Hackenberg B. Clinical utilization and practitioner preferences of orthodontic mini-implants in Romania: survey-based insights. Asian J Periodontics Orthod. 2025;5:18-32. doi:10.51847/fvnu57lTFy
36. Sallam MA, Elzoghby AO. Flutamide-loaded zein nanocapsule hydrogel, a promising dermal delivery system for pilosebaceous unit disorders. AAPS PharmSciTech. 2018;19(5):2370-82.
37. Noor H, Sabau D, Cote A, Mihetiu AF, Pirvut V, Malinescu B, et al. Advancements in esophageal stricture treatment: the role of stents in benign and malignant conditions. J Med Sci Interdiscip Res. 2024;4(2):47-52. doi:10.51847/LtuxAzRl0M
38. Schneider TL, Kruger BE. Breast cancer-specific mortality in stage IV patients with small tumors: insights from a population-based cohort. Arch Int J Cancer Allied Sci. 2025;5(2):1-12. doi:10.51847/b9vFcweAVg
39. Abdullah NA, Zulkifli MI, Mohamed AS. Refinement of the 8th AJCC staging system for medullary thyroid cancer: integrating tumor size and lymph node characteristics with SEER and multicenter validation. Arch Int J Cancer Allied Sci. 2025;5(2):34-43. doi:10.51847/R1sIaONOms
40. Lee MJ, Ferreira J. COVID-19 and children as an afterthought: establishing an ethical framework for pandemic policy that includes children. Asian J Ethics Health Med. 2024;4:1-19. doi:10.51847/haLKYCQorD
41. Negreiros AB, Ory MG. Navigating uncertain outcomes: returning genomic results in children with developmental delays. Asian J Ethics Health Med. 2024;4:20-7. doi:10.51847/grOfZd8oyo
42. Karatas KS. First episode psychotic disorder and COVID-19: a case study. Bull Pioneer Res Med Clin Sci. 2024;4(1):19-23. doi:10.51847/VP5xOKglSX
43. Figueroa-Valverde L, Marcela R, Alvarez-Ramirez M, Lopez-Ramos M, Mateu-Armand V, Emilio A. Statistical data from 1979 to 2022 on prostate cancer in populations of Northern and Central Mexico. Bull Pioneer Res Med Clin Sci. 2024;4(1):24-30. doi:10.51847/snclnafVdg
44. Belfiore CI, Galofaro V, Cotroneo D, Lopis A, Tringali I, Denaro V, et al. Studying the effect of mindfulness, dissociative experiences, and feelings of loneliness in predicting the tendency to use substances in nurses. J Integr Nurs Palliat Care. 2024;5:1-7. doi:10.51847/LASijYayRi
45. Wolderslund M, Kofoed P, Ammentorp J. Investigating the effectiveness of communication skills training on nurses' self-efficacy and quality of care. J Integr Nurs Palliat Care. 2024;5:14-20. doi:10.51847/55M0sHLo3Z
46. Piri-Gharaghie T, Beiranvand S, Riahi A, Shirin NJ, Badmasti F, Mirzaie A, et al. Fabrication and

characterization of thymol-loaded chitosan nanogels: improved antibacterial and anti-biofilm activities with negligible cytotoxicity. Chem Biodivers. 2022;19:e202100426.

47. Zhou J, Zhou L, Chen ZY, Sun J, Guo XW, Wang HR. Remineralization and bacterial inhibition of early enamel caries surfaces by carboxymethyl chitosan lysozyme nanogels loaded with antibacterial drugs. J Dent. 2025;152:105489.
48. Simpson E, Sarwar H, Jack I, Lowry D. Evaluation of the potential of chitosan nanoparticles as a delivery vehicle for gentamicin for the treatment of osteomyelitis. Antibiotics (Basel). 2024;13(3):208.
49. Raza S, Khan A, Mehmood F, Farooq U. Nationwide implementation of essential pharmacogenomic testing in the Netherlands: a decision-analytic model of lives saved and cost-effectiveness. Spec J Pharmacogn Phytochem Biotechnol. 2025;5:39-49. doi:10.51847/PUWEymkYkk
50. Musa K, Noor O, Ibrahim M, Saleh A. A validated whole-body PBPK model of dextromethorphan and its metabolites for genotype-based prediction of CYP2D6 phenotype and urinary metabolic ratio. Spec J Pharmacogn Phytochem Biotechnol. 2025;5:50-76. doi:10.51847/xbESBJHHcx
51. Ghiga I, Pitchforth E, Lundborg CS, Machowska A. Bacterial infections and antibiotic resistance in Romanian children: insights from a hospital-based study. Interdiscip Res Med Sci Spec. 2024;4(2):1-8. doi:10.51847/pISlxaQJVu
52. Kounatidis D, Dalamaga M, Grivakou E, Karampela I, Koufopoulos P, Dalopoulos V, et al. Evaluation of blood-aqueous barrier permeability in response to tetracycline antibiotics under normal and pathological conditions. Interdiscip Res Med Sci Spec. 2024;4(2):9-17. doi:10.51847/wu4fOEjgDv
53. Jagsi R, Lee J, Roselin D, Ira K, Williams J. Do U.S. medical schools follow medical associations' recommendations on paid parental leave for faculty? Ann Pharm Educ Saf Public Health Advocacy. 2025;5:1-11. doi:10.51847/r117In8wdi
54. Wong Y, Lin S, Cheng H, Hsieh T, Hsiue T, Chung H, et al. Understanding the impact of medical humanities on internship training and performance. Ann Pharm Educ Saf Public Health Advocacy. 2025;5:12-21. doi:10.51847/Z1fogzPksy
55. Keska M, Suchy W. Cardiovascular risk and systemic inflammation in rheumatoid arthritis: a comparative analysis with psoriatic arthritis. J Med Sci Interdiscip Res. 2024;4(2):30-40. doi:10.51847/PvcqitKMgB
56. Gao L, Gan H, Meng Z, Gu R, Wu Z, Zhang L, Zhu X, Sun W, Li J, Zheng Y, Dou G. Effects of genipin cross-linking of chitosan hydrogels on cellular adhesion and viability. Colloids Surf B Biointerfaces. 2014;117:398-405. doi:10.1016/j.colsurfb.2014.03.002
57. Bhatia S, Shah YA, Al-Harrasi A, Jawad M, Khan TS, Koca E, et al. Tuning the structure and physicochemical properties of sodium alginate and chitosan composite films through sodium tripolyphosphate (STPP) crosslinking. Int J Biol Macromol. 2024;264(2):130463.
58. Farkas NI, Marincas L, Barabas R, Bizo L, Ilea A, Turdean GL, et al. Preparation and characterization of doxycycline-loaded electrospun PLA/HAP nanofibers as a drug delivery system. Materials (Basel). 2022;15(6). doi:10.3390/ma15062105
59. Abosabaa SA, Arafa MG, ElMeshad AN. Hybrid chitosan-lipid nanoparticles of green tea extract as natural anti-cellulite agent with superior in vivo potency: full synthesis and analysis. Drug Deliv. 2021;28(1):2160-76.
60. Nokhodi F, Nekoei M, Goodarzi MT. Hyaluronic acid-coated chitosan nanoparticles as targeted carrier of tamoxifen against MCF7 and TMX-resistant MCF7 cells. J Mater Sci Mater Med. 2022;33(2):24.
61. Alves R, Costa B, Martins H, Faria N. Federated learning framework for adverse drug reaction prediction from multi-institutional health records. Pharmacophore. 2026;17(1):1-11. doi:10.51847/f2RnAaSwj2
62. Petrov I, Ivanova O, Smirnov D. Predicting long-acting injectable release using polymer degradation, drug loading, and microsphere morphology. Pharmacophore. 2026;17(1):33-42. doi:10.51847/MT3QwGFdub
63. Bona C, Lozano R. Delayed hematologic toxicities following axicabtagene ciloleucel and tisagenlecleucel CAR-T cell therapy: a retrospective analysis of lymphocytopenia, neutropenia, and thrombocytopenia. Asian J Curr Res Clin Cancer. 2024;4(2):1-4. doi:10.51847/13fIAq9Er0
64. Khan TM, Tahir H, Adil Q, Baig MR, Jaber AAS, Khaliel AM, et al. A three-decade overview of female-specific cancers in Malaysia: a thorough examination. Asian J Curr Res Clin Cancer. 2024;4(2):5-18. doi:10.51847/LIdazW7afN
65. Agrawal M, Shrivastava S, Khare RL, Jaiswal S, Singh P, Hishikar R. Comparative analysis of nephrotoxicity in patients on tenofovir-containing and non-tenofovir antiretroviral therapy. Ann Pharm Pract Pharmacother. 2024;4:24-33. doi:10.51847/ZTJxzvNZt4
66. Qiao J, Luo B, Ming J, Zhou S, Chen Y, Zhang X. Prevalence and implications of non-prescription antibiotic dispensing in Baghdad community pharmacies. Ann Pharm Pract Pharmacother. 2024;4:34-41. doi:10.51847/5SuGTfpren
67. Sarmout M, Xiao Y, Hu X, Rakhmetova A, Koole LH. A novel approach to achieve semi-sustained drug delivery to the eye through asymmetric loading of soft contact lenses. Heliyon. 2023;9(6):e16916.